Comparing Modeled and Measured Bathymetric Uncertainties
Effect of Doppler and Baseline Decorrelation

Haji Mohammadloo, Tannaz; Snellen, Mirjam; Amiri Simkooei, Alireza; Simons, Dick

Important note
To cite this publication, please use the final published version (if applicable).
Please check the document version above.

Comparing Modeled and Measured Bathymetric Uncertainties: Effect of Doppler and Baseline Decorrelation

1st Tannaz H. Mohammadloo
Acoustics Group, Faculty of Aerospace Engineering
Delft University of Technology
Delft, The Netherlands
T.Hajimohammadloo@tudelft.nl

2nd Mirjam Snellen
Acoustics Group, Faculty of Aerospace Engineering
Delft University of Technology
Delft, The Netherlands
M.Snellen@tudelft.nl

3rd Alireza Amiri-Simkooei
Acoustics Group, Faculty of Aerospace Engineering
Delft University of Technology
Delft, The Netherlands
A.AmiriSimkooei@tudelft.nl

4th Dick G. Simons
Acoustics Group, Faculty of Aerospace Engineering
Delft University of Technology
Delft, The Netherlands
D.G.Simons@tudelft.nl

Abstract—Nowadays Multi-Beam Echo-Sounder (MBES) derived bathymetry is used for a large range of applications. However, these measurements are affected by the uncertainties inherent to the MBES. Since the development of the depth uncertainty prediction model, MBES systems have been improved noticeably. The present contribution addresses the importance of modifying the vertical uncertainty prediction model based on the most recent insights of the error contributors.

The received signal is affected by a Doppler frequency shift due to the constant movement of the MBES. This induces an error on the beamsteering which is not corrected for by the manufacturer, and hence its contribution is a first-order effect. The phenomenon of baseline decorrelation is encountered in the MBES interferometry step in which the full MBES receiving array is divided into two sub-arrays and the phase difference of the signals arriving at these sub-arrays is determined. The slightly different angular directions of the two received signals together with the finite signal footprint reduces the coherence between them, leading to a deterioration in the precision of the MBES derived depth.

In this contribution, we compare the predictions for the bathymetric uncertainty with and without accounting for the Doppler effect and baseline decorrelation with the uncertainties estimated from real observations. To this end, data was acquired with EM2040c dual head MBES (manufactured by Kongsberg) with the center frequency of $300\,\text{kHz}$ in water depths of around $2\,\text{m}$, $10\,\text{m}$ and $30\,\text{m}$ with pulse lengths of $27\,\mu\text{s}$, $54\,\mu\text{s}$ and $134\,\mu\text{s}$ in Oosterschelde estuary, the Netherlands. In general, the predicted and measured uncertainties are in the same order of magnitude. It is seen that the contribution of the Doppler effect increases with depth and beam angle and, if not accounted for, can potentially lead to an underestimation of the total vertical uncertainty budget. Including the contribution of the baseline decorrelation improves the agreement between the modeled and measured uncertainties for the beams close to nadir.

Index Terms—Multibeam derived depth, Uncertainty prediction model, MBES inherent uncertainty, Doppler effect, Baseline decorrelation

I. Introduction

Nowadays Multi-Beam Echo-Sounder (MBES) derived bathymetry is used for a large range of applications, such as maintaining safe navigation through the production of bathymetry maps, off-shore construction and seafloor sediment classification [1], [2]. However, similar to any measured quantity, the derived depths are affected by the uncertainties inherent to the MBES. These uncertainties depend on the beam angle, uncertainties of the sensors used during the acquisition, survey configuration and operational environments. Models have thus been developed to predict the contribution of various depth uncertainty sources.

Since the development of the depth uncertainty prediction model presented by [3], [4], improvements have been realized in the MBES systems including enabling the use of Frequency Modulated (FM) pulses or adapting sophisticated bottom detection algorithms. In [5] the effect of using FM pulses on the uncertainty of the MBES derived depths is assessed. The present contribution addresses the importance of modifying the vertical uncertainty prediction model based on the most recent insights of the error contributors considering only Continuous Wave (CW) pulse shape.

The constant movement of the MBES affects the received signal through a Doppler frequency shift inducing an error on the beamsteering. This gives rise to an uncertainty in the estimated depth. The induced uncertainty in the beam steering is not corrected for by the manufacturer, and hence it is a first-order effect. In this paper, this error source is accounted for by introducing an additional term to the equation describing the random depth error due to the uncertainty in the roll and steering angle [5].

The phenomenon of baseline decorrelation is encountered in

the MBES interferometry step in which the full MBES receiving array is divided into two sub-arrays and the phase difference of the signals arriving at these sub-arrays is determined. The arrival time is considered to be the time corresponding to the zero phase difference. Due to the slightly different angular directions of the two received signals and the finite signal footprint (giving rise to a directivity in the scattered signal), their coherence is reduced and the quality of the MBES derived depth is negatively affected. Accounting for this term requires replacing the existing expression for uncertainties in the angle of impact with an expression reflecting the errors in the time estimate due to the baseline decorrelation (function of a number of parameters including the standard deviation of the phase difference between the two sub-arrays). Accounting for these contributors in the uncertainty prediction model provides one with a more realistic description of the uncertainties. The required modifications of the uncertainty prediction models have been discussed in detail in [5]. Reference [6] proposed a unified definition of the so-called quality factor for sonar bathymetry measurements which is the estimate of the local depth-relative error. This quality factor is linked to the acoustical signal processing and is thus only a component of the total quality of the sounding.

Here, the depth uncertainty predictions with (using the modifications presented in [5] to the original model presented by [3], [4]) and without (based on the original model) accounting for the baseline decorrelation and Doppler effect on beamsteering are compared to those estimated from real observations. To this end, three data sets acquired in water depths of around $2\,\mathrm{m}$, $10\,\mathrm{m}$ and $30\,\mathrm{m}$ with pulse lengths of $27\,\mathrm{\mu s}$, $54\,\mathrm{\mu s}$ and $134\,\mathrm{\mu s}$, in Oosterschelde estuary, the Netherlands, were analyzed. Having these measurements allows for experimentally investigating the effect of water depth on the uncertainties and to compare the measured trends with those predicted.

The present contribution is organized as follows. Section II presents the approach used for depth uncertainty calculation along with the modifications required to account for the contributions of the baseline decorrelation and Doppler effect. A description of the data sets used is given in Section III followed by the results in Section IV. The conclusions are given in Section V.

II. METHODOLOGY

As mentioned, for the depth uncertainty prediction, use is made of the model presented in [3], [4]. This model is developed assuming independent sources of uncertainty, two-layer sound speed in the water column and flat seafloor. The depth d below the transducer is then derived as

$$d = r \cos P \cos(\theta_s + R + \theta_{\mathrm{mount}}) = r \cos P \cos \theta \quad (1)$$

where θ_s is the steering angle relative to the transducer normal. P is the pitch angle, R is the roll, and θ_{mount} is the across track angle under which the MBES is mounted on the ship, see Fig. 1. The angle θ is defined as $\theta_s + R + \theta_{\mathrm{mount}}$ and is
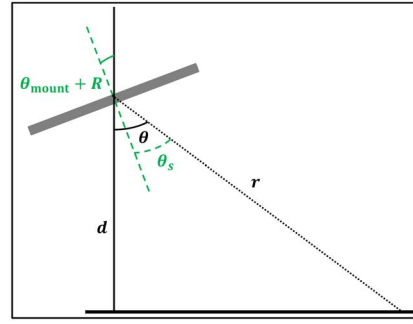

Fig. 1. Shematic of the MBES array, showing parameters relevant for estimating the depth in (1).

the beam angle with respect to the depth-axis. r is the oblique distance between the transducer and seafloor.

The bathymetric uncertainty sources are categorized as
1) Echosounder contribution, $\sigma_{d_1}^2$, due to the erros in the measurements of the travel time of the signal, speed of sound and angle of impact of the incoming sound wave at the MBES transducer.
2) Angular motion sensor contribution, $\sigma_{d_2}^2$, due to the errors in the roll and pitch measurements and imperfectness of their corrections.
3) Motion sensor and transducer alignment contribution, $\sigma_{d_3}^2$, due to the discrepancies between the roll and pitch angle measurements at the motion sensor and the transducer.
4) Sound speed contribution, $\sigma_{d_4}^2$, due to the sound speed errors at the transducer array and those of the water column.
5) Heave contribution, $\sigma_{d_5}^2$, due to the errors in the heave measurements and those induced from roll and pitch errors.

The total depth error is then derived as

$$\sigma_d^2 = \sqrt{\sigma_{d_1}^2 + \sigma_{d_2}^2 + \sigma_{d_3}^2 + \sigma_{d_4}^2 + \sigma_{d_5}^2} \quad (2)$$

Here, we do not present all the equations and an interested reader might refer to [3], [4]. However, we will discuss the ambiguity that occurs in the interpretation of some existing equations. We also present the modification required to account for the baseline decorrelation and Doppler effect on beamsteering.

A. Range Sampling Resolution

The random depth error due to uncertainty in the measured distance, i.e., part of echosounder contribution ($\sigma_{d_1}^2$), r_{meas} is given by

$$\sigma_{d_{r_1}}^2 = (\cos P \cos \theta)^2 \sigma_{r_{meas}}^2 \quad (3)$$

r_{meas} depends on the type of MBES and is affected by both sampling resolution and pulse length and follows from

$$\sigma_{r_{\mathrm{meas}}}^2 = \left(\frac{\triangle r_s}{2}\right)^2 + \left(\frac{c\tau}{4}\right)^2 \quad (4)$$
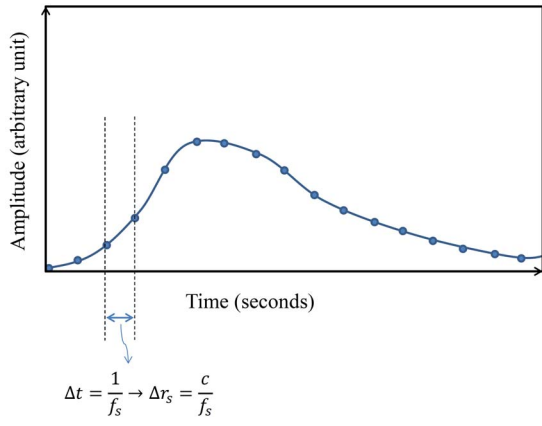
Fig. 2. A schematic example of the received signal by the individual transducers and the finite sampling.

where $\triangle r_s$ and $c\tau$ are the range sampling resolution and the pulse length in meter, respectively. The first term reflects the uncertainty induced due the fact that a finite sampling is used for sampling the signals as received by the individual transducers, see Fig. 2. There are a number of issues that come with this term:

1) This range sampling resolution term is often mixed up with the term range resolution, i.e., $\frac{\tau c}{2}$. The latter reflects that all dots indicated in Fig. 2 do not stem from a single point on the sediment, but from the signal footprint that increases with increasing pulse length. This term is also accounted for in the calculations of the depth random error, see the second term in (4).

2) Another issue related to the range sampling resolution, is the sampling frequency. The reported value for this parameter is the output sampling frequency which is different from the one used for applying the bandpass filters and beamforming with the latter being higher. Knowledge of this value is required. For sampling frequencies in the order of MHz, the contribution of the first term in (4) becomes negligible.

3) The term used for describing the error in the range measurements in (4) is often considered to result in predicting too high uncertainties [3]. Therefore, this term is scaled by 0.707 compared to [4].

For the current study, due to the lack of knowledge regarding the relevant sampling frequency, it was decided to choose the maximum output sample rate of EM2040c equalling $60\,\mathrm{kHz}$ for the predictions. Assuming a constant sound speed of $1515\,\mathrm{m/s}$ in the water column, which is a valid assumption for the surveyed areas, the range sampling resolution is equal to $\triangle r_s = \frac{c}{f_s} = 0.025\mathrm{m}$. Considering issue 1 addressed in this section, also the range resolution is calculated. For the pulse lengths of $27\,\mathrm{\mu s}$, $54\,\mathrm{\mu s}$ and $134\,\mathrm{\mu s}$ the range resolution is $0.020\,\mathrm{m}$, $0.041\,\mathrm{m}$ and $0.101\,\mathrm{m}$, respectively. Especially for the longest pulse length, the range resolution is significantly larger than the range sampling resolution. This indicates that if one uses the range resolution instead of the range sampling

resolution, the depth uncertainties can be either overestimated or underestimated. To illustrate this, the predicted depth uncertainties are shown in Fig. 3 for water depths of $2\,\mathrm{m}$ and $30\,\mathrm{m}$ and with the shortest and longest pulse length using the range sampling resolution, see the black curves, and the range resolution, see the green curves. As can be seen, for the shortest pulse length, the difference is in the order of a few millimeters and an underestimation occurs in case of using range resolution as it gets smaller than the range sampling resolution. However, as the pulse length increases, the difference gets larger and using the range resolution leads to an overestimation. For the remaining part of this contribution, the predictions are given using the range sampling resolution based on a sample frequency of $60\,\mathrm{kHz}$.

B. Accounting for most recent insights in contributors to MBES depth uncertainties: Doppler effects and baseline decorrelation

The constant movement of the MBES affects the received signal through a Doppler frequency shift. This is translated to an uncertainty in the steering angle, $\sigma^2_{d,\theta_{\mathrm{Doppler}}}$, giving rise to uncertainties in the estimated depths. The following expression holds for the induced bias in the beamsteering due to the Doppler effect, [5], [7],

$$\delta\theta_s \approx -\frac{v_r}{c}\tan\theta \tag{5}$$

where v_r and c are the speed of the array center at reception and speed of the sound in the water column, respectively. This bias is irrespective of the pulse type. In contrast to the effect of Doppler on matched filtered signals (encountered when using FM pulse type) which is often take into account in the post processing, the Doppler effect on beam steering is not accounted for. Its contribution to the depth uncertainty has thus a first-order effect and is derived assuming v_r as a random variable. Following [5], the expression for the contribution of this error is

$$\sigma^2_{d,\theta_{s,\mathrm{Doppler}}} = (r\cos P\sin\theta)^2\sigma^2_{\theta_{s,\mathrm{Doppler}}}$$
$$= (r\cos P\sin\theta)^2\frac{\mathrm{var}(v_r)}{c^2}\tan^2\theta \tag{6}$$

where c is the sound speed at the MBES transducer. $\mathrm{var}(v_r)$ denotes the variations in the speed of the array center at the reception, which depends on the sea-state.

The phenomenon of baseline decorrelation is encountered in the MBES interferometry step. This is due to combined effect of (fluctuating) directivity pattern of the signal footprint (resulting from contribution of all scatterers within it) and a slightly different angular direction of the received signal from the bottom as sensed by the two sub-arrays used in the interferometry step. The coherence between the two received signals is reduced leading to a degradation in the quality of the phase estimate. The contribution of the baseline decorrelation to the random depth uncertainty ($\sigma^2_{d,t_{\mathrm{Decorr}}}$), [5], [7], is

$$\sigma^2_{d,t_{\mathrm{Decorr}}} = \frac{(d\sigma_{\triangle\phi})^2}{\left(2\pi f_c\frac{L\cos\theta}{c\tan\theta}\right)^2 N} \tag{7}$$
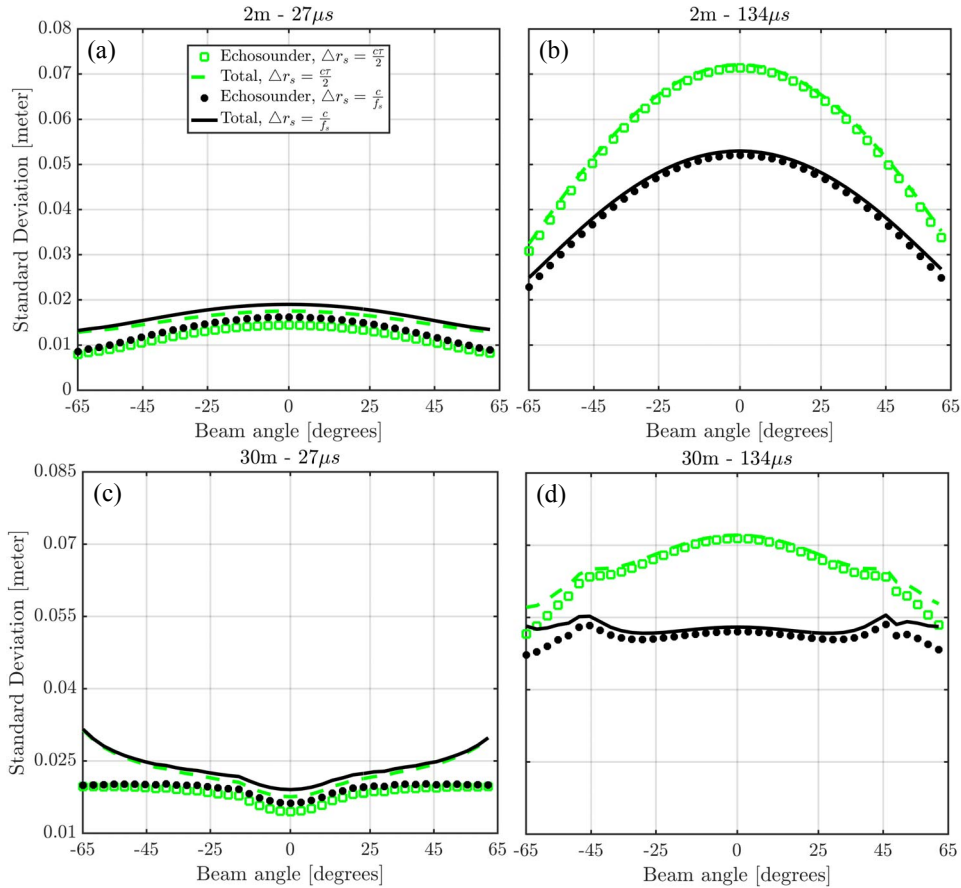
Fig. 3. Echosounder contribution to the depth uncertainty (green squares and black asterisks) and that of the total (green dashed and black solid) derived using $\triangle r_s = \frac{c\tau}{2}$ (green) and $\triangle r_s = \frac{c\tau}{f_s}$ (black) for the water depths of $2\,\mathrm{m}$, (a) and (b), and $30\,\mathrm{m}$ (c) and (d).

where $\sigma^2_{\triangle\phi}$ is the uncertainty in the estimate of the phase difference between the two sub-arrays [8]. f_c and L are the center frequency and the baseline length respectively, i.e., one-third of the theoretical array length corrected for the shading [7].

The current expressions for the the vertical uncertainty do not account for the Doppler effect on beamsteering. However, the baseline decorrelation is accounted for in an approximate way, not accounting for the specific pulse characteristics. Here it will be investigated to what extent these two factors affect the model-data comparison.

III. DATA SETS DESCRIPTION

A survey was carried out by Rijkswaterstaat in the Oosterschelde estuary (Eastern Scheldt), the Netherlands. The Kongsberg EM2040c dual head MBES with CW pulse type was used, see [9]. The port and starboard mounting angles of EM2040c were around $40°$. The survey was carried out in three different depths of around $2\,\mathrm{m}$, $10\,\mathrm{m}$ and $30\,\mathrm{m}$ enabling the assessment of the depth on the vertical uncertainties, see Fig. 4 derived from Qimera, considering a cell size of $0.25\mathrm{m} \times 0.25\mathrm{m}$. Both Equiangular and Equidistant beam spacing modes were used to investigate their impact. Moreover, to increase the density of soundings, dual swath acquisition mode was enabled.

The sound velocity profiler was manufactured by AML oceanographic and its accuracy, indicated by the manufacturer, is around $0.02\,\mathrm{m/s}$, [10]. However, from measurements in different locations (inland waterways and the North Sea), the uncertainty was found to be $0.2\,\mathrm{m/s}$ and hence this value is chosen as a more realistic description of the systems uncertainty and will be used later on when modelling the depth uncertainty induced by the uncertainty in the sound speed profile.

Using QINSy (Quality Integrated Navigation System developed by Quality Positioning Service (QPS) BV) for data acquisition and receiving a correction signal from Real Time Kinematic (RTK) service means that the depth relative to the chart/vertical datum is directly measured and accounting for height offsets is not necessary. However, heave measurements are used for to calculate the height of the vessel's center of gravity between two position updates, and thus its uncertainty is of importance as it contributes to the depth uncertainty.

It should be highlighted that the uncertainty prediction model is based on the uncertainties inherent to the MBES and systematic error sources have not been considered. The degradation in quality of the MBES depth measurements is not solely due to the former, but systematic errors also contribute.
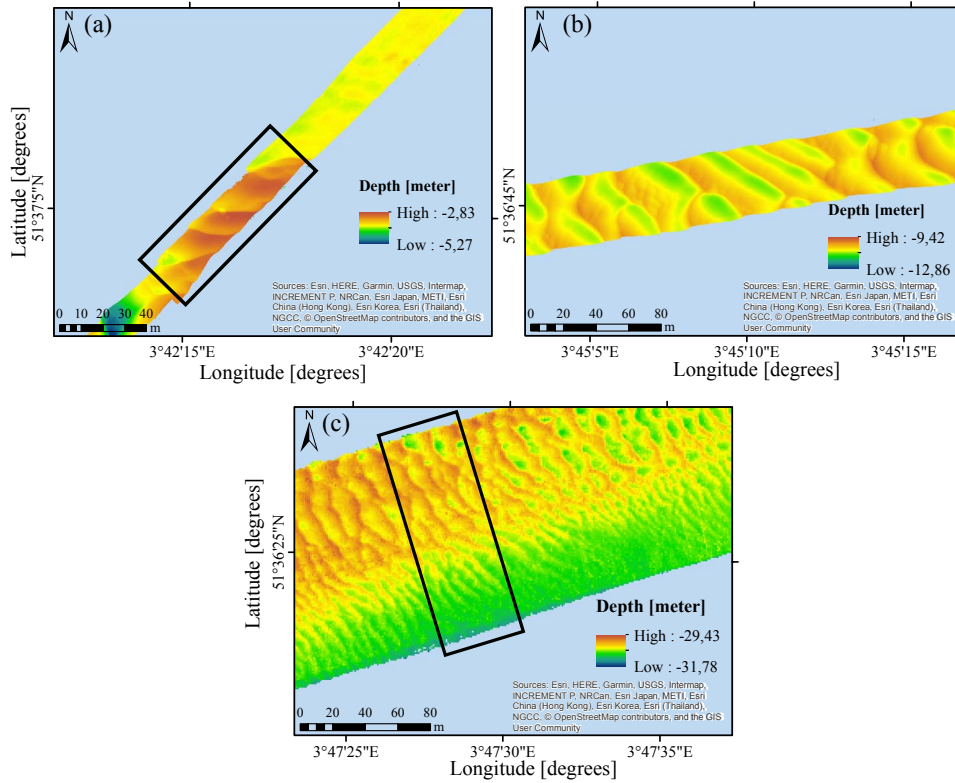
Fig. 4. Bathymetry map of the surveyed areas in water depth of $2\,\mathrm{m}$, (a), $10\,\mathrm{m}$, (b), and $30\,\mathrm{m}$, (c), using the measurements with a pulse length of $54\,\mathrm{\mu s}$ and equidistant beamspacing mode.

This contributor can be categorized as static and dynamic ones. The former include (not limited to) the relative heading, pitch and roll misalignments between the MBES and Inertial Navigation Sensor, see [11] for a detailed discussuion. The correction of these systematic errors if of importance and done using the patch test. For the three surveyed areas considered, the patch test was carried out, and these systematic errors (if present) have been thus excluded. As for the dynamic systematic errors, they can be identified using the correlation analysis between the motion time series and depth derivatives, [12]. The data have been carefully examined and the signatures of such errors have not been found.

IV. RESULTS

Shown in Fig. 5 are the maps of the measured vertical standard deviation for the three different surveyed areas, i.e., water depths of $2\,\mathrm{m}$, (a) $10\,\mathrm{m}$, (b) and $30\,\mathrm{m}$, (c). These maps are based on the measurements with a pulse length of $54\,\mathrm{\mu s}$ and equiangular beamspacing mode. These maps provide one with the possibility to assess the variations of the standard deviation within the full surveyed area with the same cell size as the bathymetry maps.

For the area with a water depth of $2\,\mathrm{m}$, a large standard deviation for a relatively broad range of beams (proportional to the swath width) around the nadir is seen, followed by a decrease towards the outer beams. Also visible is the impact of morphological features on the standard deviation. For example,

varying morphology in the South-West of the area with $2\,\mathrm{m}$ water depth indicated by the black rectangle, see Fig. 4(a), increases the standard deviation. Considering a similar plot for the measurements in the area with $10\,\mathrm{m}$ of water depth, Fig. 5(b), again a dependency on the beam angle (location in the swath) is observed (as also seen in [13]). However, having a larger standard deviation occurs for a smaller part of the swath in proportion to the swath width than for the case with $2\,\mathrm{m}$ of water depth. Also for the deepest area surveyed, again a dependency on the beam angle is seen, though for a smaller proportion of the swath compared to the shallower depths.

As mentioned, the data was acquired in equidistant and equiangular beam spacing modes. For the former, the beam angles are adjusted to give an equal distance between the points sensed on the seafloor. As for the equiangular, the beams are adjusted such that they have equal angular spacing, see [14] for a detailed discussion. The equiangular beam spacing mode provides many soundings close to the center of the survey line, but fewer towards the outer swath compared to the equidistant spacing mode. From theory, no effects of the beam spacing mode on the depth uncertainties are expected. However, to validate this expectation also for the real data, the measured uncertainties for the two spacing modes and for the pulse length of $27\,\mathrm{\mu s}$ are shown in Fig. 6 for water depths of $2\,\mathrm{m}$, (a), and $10\,\mathrm{m}$, (b) for 50 consecutive pings. It is seen that the measured standard deviation for both modes almost coincide. Therefore, for the remaining part of this report the
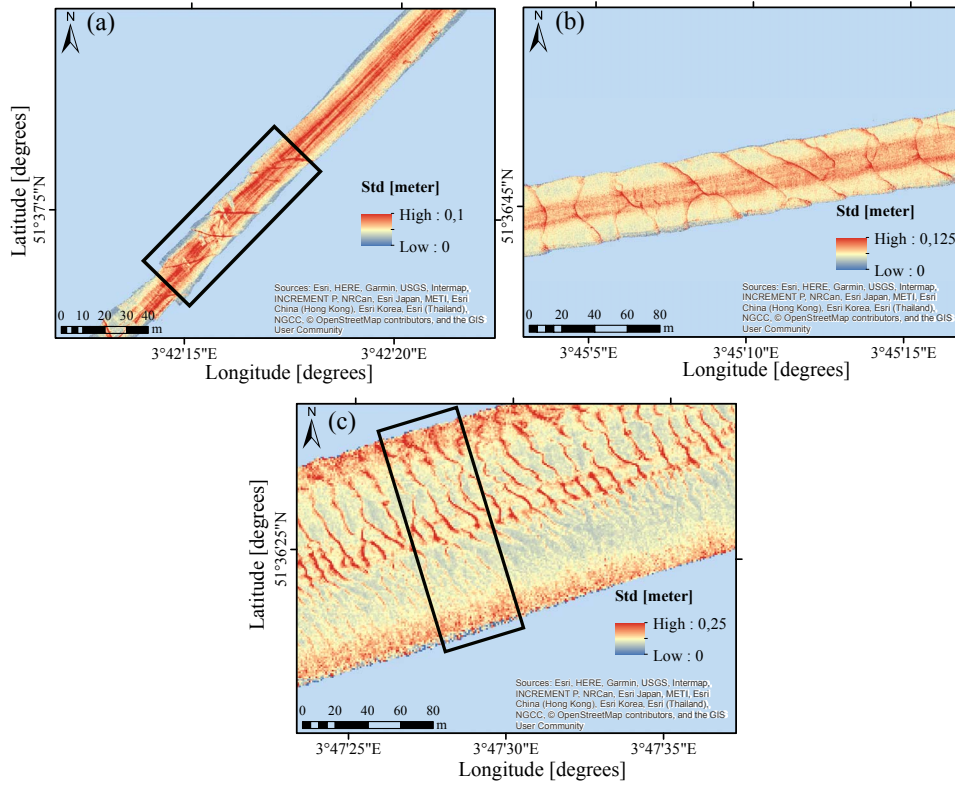
Fig. 5. Map of the measured depth standard deviation of the surveyed areas in water depth of $2\,\mathrm{m}$, (a), $10\,\mathrm{m}$, (b) and $30\,\mathrm{m}$, (c), using the measurements with the pulse length of $54\,\mu\mathrm{s}$ and equiangular beamspacing mode.
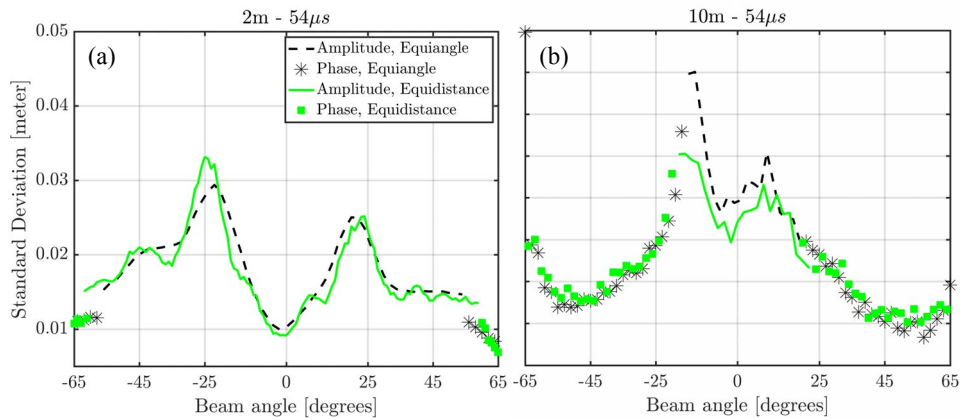
Fig. 6. Estimate of the vertical uncertainty derived from the measurements for the water depth of (a) $2\,\mathrm{m}$ and (b) $10\,\mathrm{m}$ with equiangular (black) and equidistance (green) beamspacing modes. The change from amplitude to phase detection is shown by the asterisks and squares respectively.

results shown are for the equidistance beam spacing mode.

A. Accounting for the baseline decorrelation and Doppler effect

To investigate the impact of accounting for the Doppler effect on beamsteering and baseline decorrelation on the uncertainty prediction budget, a small area consisting of around 50 pings is considered. This limited number of pings decreases the effect of bottom morphology and still provides a robust estimate of the standard deviation. As mentioned in Section

II, predictions are based on the assumption of a flat seafloor. However, in reality this assumption is easily violated, and hence larger uncertainties are obtained due to the non-flatness of the bottom. As an example, in case of having a steep slope, the standard deviation of the depth measurements is affected by both uncertainties inherent to the MBES and the slopes. Here, the contribution of the morphology is accounted for by fitting a bi-quadratic or linear (depending on the morphology) function to the depth measurements within a surface patch consisting of a few pings and beams in the

Step1: Vertical uncertainty prediction model of Hare, [3]

Step2: Model of Step 1 is modified to account for the baseline decorrelation and Doppler effect

Step3: Model of Step 2 is further modified to account for the additive noise assuming a soft sediment
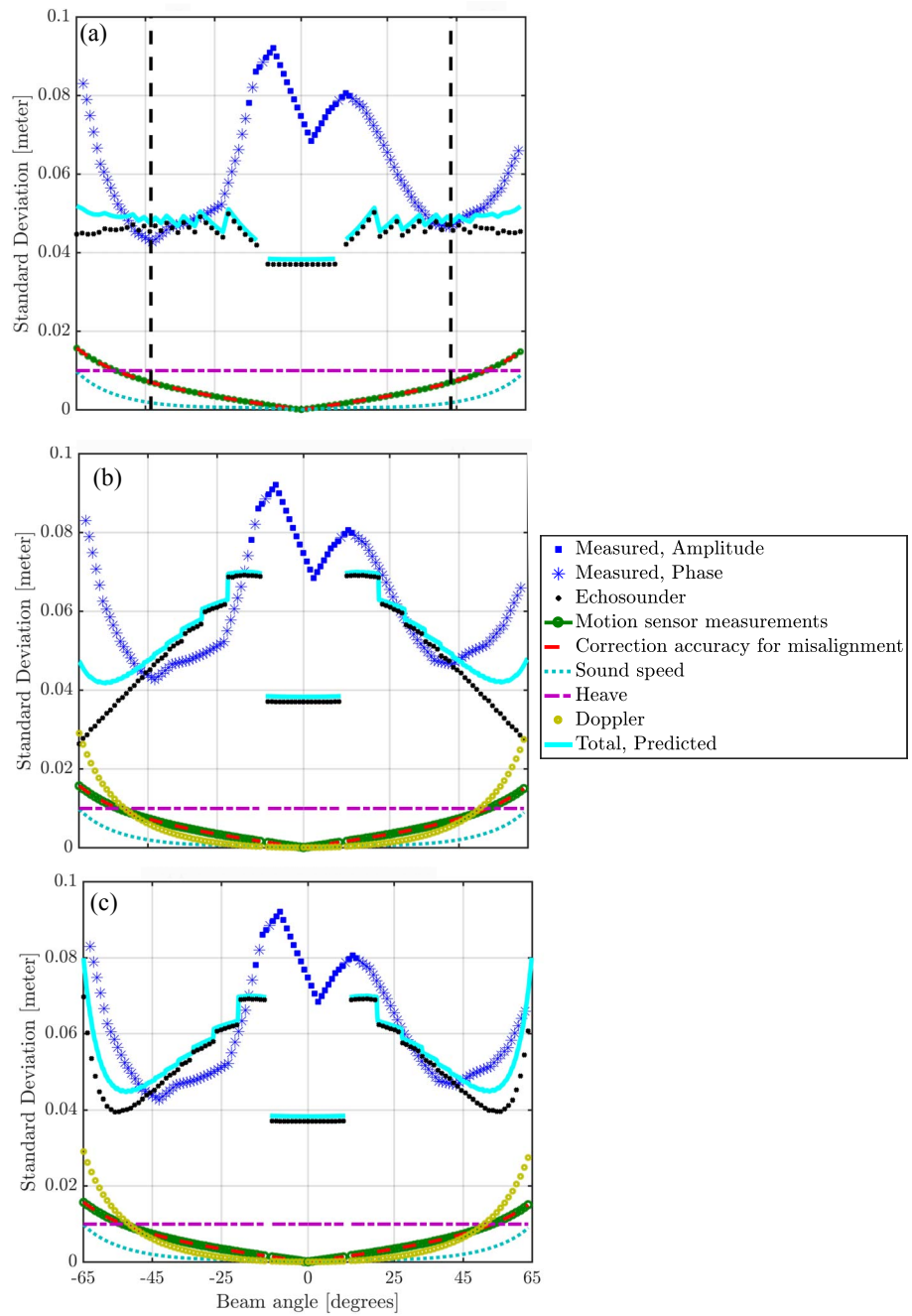
Fig. 7. Measured vertical standard deviation (blue) and those predicted without accounting for the contributions of baseline decorrelation and Doppler effect, (a), accounted for the contributions of baseline decorrelation and Doppler effect, (b), accounted for the contributions of baseline decorrelation, Doppler effect and additive noise for the water depth of 30 m and the pulse length of 134 μs. The change from amplitude to phase detection is shown in by switching from square markers to asterisk markers with the same color.

along- and across-track directions respectively, see [15]. The least-squares estimate of the variance can be then calculated using the residuals of the depth measurements from the surface fitted.

Shown in Fig. 7 are the measured and predicted depth uncertainties for a water depth of 30 m with a pulse length of 134 μs for the situation where the contributions of the Doppler effect and baseline decorrelation have not been taken into account, 7(a); 7(b) illustrates the predictions considering these uncertainty sources, see (6) and (7). The contribution of the Doppler effect is shown by the green circles. As for the baseline decorrelation, it is now considered within the echosounder contribution. As seen, the contribution of the Doppler effect increases with beam angle and does not depend on the pulse length. However, the contribution of the baseline decorrelation decreases with beam angle and it does depend

on the pulse shape.

Compared to the case where these contributions were not considered, (a), the agreement between the modelled and measured uncertainties is improved for the beams closer to the nadir and has not changed noticeably for the remaining part of the swath. Similar to the situation where the baseline decorrelation and Doppler effect were not considered, the model underestimates the vertical uncertainties for the outer beams. A potential approach for improving the agreement between the predicted and measured uncertainties for the outer beams is to account for the contribution of the additive noise. The nature of the additive noise makes its predictions complicated, see [16], requiring information on the acoustic backscatter returned to the MBES. The backscatter strength returned to the sonar is the result of a complex interaction of the acoustic pulse transmitted and the often inhomogeneous seafloor, [17], and might not be known before the data acquisition and no closed form expressions can be derived. However, here we have investigate the contribution of additive noise assuming a fine sediment (representative of the surveyed area). The predicted depth uncertainties accounted for the contribution of the additive noise in addition to the other sources inherent to the MBES is shown in 7(c). As seen, the agreement between the predicted and measured uncertainties is now also improved for the beams way from nadir.

V. Conclusions

Predicting the uncertainty in MBES bathymetric measurements is nowadays an important and almost standard step in the planning of MBES surveys and models have thus been developed. These models enable one to assess whether the required survey standards can be met in a specific measurement campaign for a given combination of measurement equipment, MBES settings and water depth.

Since the development of the depth uncertainty prediction, MBES systems have been improved from different perspectives. Moreover, new insights into the uncertainty sources affecting the quality of depth measurements are obtained, such as the baseline decorrelation, Doppler effect and additive noise consideration. The present contribution addresses the importance of modifying the vertical uncertainty prediction model based on the most recent insights of the error contributors.

The standard deviation of the depth measurements in water depth of $2\,\mathrm{m}$, $10\,\mathrm{m}$ and $30\,\mathrm{m}$ is in general larger for the beams closer to nadir. As the depth increases, the proportion of the swath in which the vertical depth standard deviation is larger for the inner beams decreases. There is a strong dependency between the measured standard deviation and the bottom morphology, and thus its effect has to be taken into account. The comparison between the modelled and measured uncertainties with and without taking the baseline decorrelation and Doppler effect into account in the uncertainty model, indicates that accounting for these uncertainty sources improves the model-data agreement particularly for inner parts of the swath. Further improvement of the model can be done by considering the uncertainty induced by additive noise, which depends on the bottom characteristics. It is shown that for a soft sediment (representative of the surveyed areas) accounting for this contributor improves the model-data for the outer parts of the swath to a noticeable extent.

References

[1] T. J. Anderson, C. Syms, D. A. Roberts and D. F. Howard, "Multi-scale fish-habitat associations and the use of habitat surrogates to predict the organisation and abundance of deep-water fish assemblages," J. Exp. Mar. Biol. Ecol. vol. 379 (1-2), pp. 34–42, 2009.

[2] G. Di Maida, A. Tomasello, F. Luzzu, A. Scannavino, M. Pirrotta, C. Orestano and S. Calvo, "Discriminating between Posidonia oceanica meadows and sand substratum using multibeam sonar," ICES J. Mar. Sci., vol. 68(1), pp. 12–19, 2011.

[3] R.Hare, "Error Budget Analysis for US Naval Oceanographic Office (NAVOCEANO) Hydrographic Survey Systems," Hydrographic Science Research Center (HSRC), Mississippi, USA, 2001.

[4] R.Hare, "Depth and Position Error Budgets for Multibeam Echosounding," Int. Hydrogr. Rev., vol. LXXII(2), pp. 37–69, 1995.

[5] T. H. Mohammadloo, M. Snellen and D. G. Simons, "Multi-beam echosounder bathymetric measurements: Implications of using frequency modulated pulses," J. Acoust. Soc. Am., vol. 144(2), pp. 842–860, 2018.

[6] X. Lurton and J. M. Augustin, "A Measurement Quality Factor for Swath Bathymetry Sounders," IEEE J, Oceanic. Eng, vol. 35(4), pp. 852–862, 2010.

[7] P. Vincent, "Modulated signal impact on multibeam echosounder bathymetry," Ph.D dissertation, Télécom Bretagne Sous En habilitation conjointe avec lUniversité de Rennes 1, 2013.

[8] R. J. A. Tough, D. Blacknell, and S. Quegan, "A statistical description of polarimetric and interferometric synthetic-aperture radar data," Proc. R. Soc. London Ser. A, vol. 449(1937), pp. 567–589, 1995.

[9] Kongsberg Maritime, "EM2040C," available at textthttps://www.kongsberg.com, 2016.

[10] AML Oceanographic, "SV & CTD Profilers: Base.X2 and Minos.X," available at `https:599//amloceanographic.com`, 2017.

[11] A. Godin, "The calibration of shallow water multibeam echo-sounding systems," MS.c thesis, Department of Geodesy and Geomatics Engineering, University of New Brunswick, 1998.

[12] J. E. Hughes Clarke, "Dynamic motion residuals in swath sonar data : Ironing out the creases," Int. Hydrogr. Rev., 4(1), 6–23.

[13] T. H. Mohammadloo, M. Snellen, D. G. Simons, B. Dierikx and S. Bicknese, "Case Study on the use of Alternatives for Determining the Shallowest Depth for Bathymetric Charting," J Surv. Eng., in press, 2019.

[14] J. E. Hughes Clarke, J. V. Gardner, M. Torresan and L. Mayer, "The limits of spatial resolution achievable using a 30 kHz multibeam sonar: model predictions and field results," IEEE Oceanic Engineering Society. OCEANS'98. Conference Proceedings (Cat. No.98CH36259), Nice, France, pp. 1823–1827 vol.3, 1998.

[15] A. Amiri-Simkooei, M. Snellen, and D. G. Simons, "Riverbed sediment classification using multi-beam echo-sounder backscatter data," J. Acoust. Soc. Am., 126(4), pp. 1724–38, 2009.

[16] X. Lurton, "An Introduction to Underwater Acoustics: Principles and Applications," 2nd ed. (Springer, Berlin), 2010.

[17] D. D. Sternlicht and C. P. de Moustier, "Time-dependent seafloor acoustic backscatter (10100 kHz)," J. Acoust. Soc. Am., 114(5), pp. 2709–2725, 2003.